

CALCIUM CURRENT IN ISOLATED NEONATAL RAT VENTRICULAR MYOCYTES

BY NERI M. COHEN AND W. J. LEDERER

From the Department of Physiology, University of Maryland at Baltimore, School of Medicine, 660 West Redwood Street, Baltimore, MD 21201, U.S.A.

(Received 18 November 1986)

SUMMARY

1. Calcium currents (I_{Ca}) from neonatal rat ventricular heart muscle cells grown in primary culture were examined using the 'whole-cell' voltage-clamp technique (Hamill, Marty, Neher, Sakmann & Sigworth, 1981). Examination of I_{Ca} was limited to one calcium channel type, 'L' type (Nilius, Hess, Lansman & Tsien, 1985), by appropriate voltage protocols.

2. We measured transient and steady-state components of I_{Ca} , and could generally describe I_{Ca} in terms of the steady-state activation (d_{∞}) and inactivation (f_{∞}) parameters.

3. We observed that the reduction of I_{Ca} by the calcium channel antagonist D600 can be explained by both a shift of d_{∞} to more positive potentials as well as a slight reduction of I_{Ca} conductance. D600 did not significantly alter either the rate of inactivation of I_{Ca} or the voltage dependence of f_{∞} .

4. The calcium channel modulator BAY K8644 shifted both d_{∞} and f_{∞} to more negative potentials. Additionally, BAY K8644 increased the rate of inactivation at potentials between +5 and +55 mV. Furthermore, BAY K8644 also increased I_{Ca} conductance, a change consistent with a promotion of 'mode 2' calcium channel activity (Hess, Lansman & Tsien, 1984).

5. We conclude that, as predicted by d_{∞} and f_{∞} , there is a significant steady-state component of I_{Ca} ('window current') at plateau potentials in neonatal rat heart cells. Modulation of the steady-state and transient components of I_{Ca} by various agents can be attributed both to specific alterations in d_{∞} and f_{∞} and to more complicated alterations in the mode of calcium channel activity.

INTRODUCTION

Steady-state calcium currents should exist over plateau potentials in heart muscle. This prediction stems from both analysis of calcium currents in ventricular muscle (McDonald, Pelzer & Trautwien, 1984), Purkinje fibres (Kass & Sanguinetti, 1984; Lee, Marban & Tsien, 1985; Sanguinetti, Krafte & Kass, 1986), sino-atrial node preparations (Brown, Kimura, Noble, Noble & Taupignon, 1984) and single cells (Mitchell, Powell, Terrar & Twist, 1983; Josephson, Sanchez-Chapula & Brown, 1984; Sanguinetti *et al.* 1986) and patch-clamp analysis of single-calcium-channel

currents (Cavalie, Ochi, Pelzer & Trautwein, 1983; McDonald, Cavalie, Trautwein & Pelzer, 1986). Calcium channel modulation by various drugs has been investigated using both 'whole-cell' and single-channel techniques. Hess, Lansman & Tsien (1984) found that the calcium channel agonist BAY K8644 increases I_{Ca} by stabilizing the channel in a 'conducting' mode (mode 2) while Sanguinetti *et al.* (1986) explained similar observations by altering a single rate constant in a three-state kinetic model. Cavalie, Pelzer & Trautwein (1985) found that D600 decreases I_{Ca} by increasing the mean single-channel closed time. Direct comparisons between the results in the above experiments are complicated, however, because (1) different species were generally used (guinea-pig, rat, rabbit, cat and calf); (2) the experiments were performed at different temperatures (20–37 °C) and (3) different divalent current carriers (usually Ba^{2+} or Sr^{2+} and only rarely Ca^{2+}) were used. We undertook the experiments described in this paper in order to examine directly the relationship between currents predicted by activation and inactivation properties of I_{Ca} and the measured steady-state and transient I_{Ca} . Additionally, we used two agents (D600 and BAY K8644) known to modulate I_{Ca} to test the utility of the analysis methods employed.

We have used the 'whole-cell' voltage-clamp technique (Hamill, Marty, Neher, Sakmann & Sigworth, 1981) in primary cultures of single neonatal heart cells. We used Ca^{2+} as the current carrier and all experiments were carried out at room temperature (22 °C) in order to slow I_{Ca} . We have found that the voltage dependence of the steady-state current corresponds to the voltage dependence of the overlap of d_{∞} and f_{∞} and leads to the presence of a calcium 'window current' analogous to the sodium 'window current' described by others (cf. Attwell, Cohen, Eisner, Ohba & Ojeda, 1979; Colatsky, 1982). We conclude that the steady-state variables (d_{∞} and f_{∞}) are valuable in describing the voltage dependence of both the steady-state and (surprisingly) the transient components of I_{Ca} . Furthermore, much of the modulation of I_{Ca} by D600 and BAY K8644 can be explained by changes in d_{∞} and f_{∞} . A preliminary account of these results has been presented to the Biophysical Society (Cohen & Lederer, 1986).

METHODS

Single-cell isolation procedure

Neonatal (2–7 days old) rat hearts were rapidly removed from the chest cavity of anaesthetized animals and rinsed in filter-sterilized calcium-free dissociation solution containing (in mM): NaCl, 140; KCl, 4; glucose, 10; HEPES, 10 (pH 7.4), and bovine albumin (1 g/l; Miles Laboratories Fraction V). After mincing in 4.0 ml of the same solution containing collagenase (1 mg/ml; Sigma type II-S), the tissue fragments were incubated at 37 °C for 1 h. At the end of the incubation period the cell suspension was triturated with a blunt Pasteur pipette and suspended in culture medium (see below).

Culture procedure

Prior to cell isolation No. 1 glass cover-slips were scored and cut into pieces approximately 0.5 × 1.25 mm and flame sterilized. These pieces were placed in a small (35 mm) tissue-culture dish (Falcon 3001) covering about 70% of the bottom of the dish and exposed to ultra-violet light for 1 h. Cells were isolated as described above and 1.0 ml of the triturated cell suspension was plated into 2.0 ml of Dulbecco's Modified Eagle's Medium (DMEM) (GIBCO) containing 10% Cadet Calf Serum (CCS) (Biocell 2003) in the prepared tissue-culture dish. The cells were incubated at 37 °C

in a CO₂ incubator (5% CO₂-95% O₂; pH 7.4) and 24 h after plating the media was aspirated and replaced with standard 10% CCS-DMEM. By day 2 of culture, sufficient single cells had adhered to the cover-glass so that experiments could be performed. Experiments were carried out between day 2 and day 4 in culture.

Experimental procedure

Glass pieces with adherent cells was removed from the tissue-culture dish, transferred to the experimental chamber and superfused at 1 ml/min with a modified Tyrode solution containing (in mM): NaCl, 145; KCl, 4; CaCl₂, 1; MgCl₂, 1; glucose, 10; HEPES, 10 (pH 7.36), and 10 μM-tetrodotoxin (TTX; Sigma). Patch electrodes were pulled (BB-CH Mechanex, Geneva) from glass capillaries (1.5 mm, WPI No. 1B150F-6) to a tip diameter of < 1 μm and resistance of 4-6 MΩ when filled with (in mM); potassium glutamate, 129; CsCl, 20; NaCl, 1; and 10 μM-EGTA. Possible errors introduced by pipette series resistance (measured as the time constant of the uncompensated capacity transient divided by the cell capacity (43 ± 6.7 pF)) were compensated by using dynamic series resistance control compensation to provide the fastest possible capacity transient without ringing; there remained an additional 2-3 MΩ uncompensated series resistance. Experiments were performed in the 'whole-cell' voltage-clamp configuration (Hamill *et al.* 1981) at 22 °C. With sodium and potassium channels blocked by external TTX and internal caesium, respectively, voltage-clamp pulses (Dagan 8900; feed-back resistor 1 GΩ) were applied to investigate the calcium current (I_{Ca}). Data was stored either on FM tape (Vetter Model D) or video tape (Sanyo VCR7200) after digitization (Sony digital audio processor PCM-501ES) (Bezanilla, 1985).

Curve-fitting procedure

Data was analysed off-line with a portable personal computer (Compaq Computer Corp., Houston, TX, U.S.A.) and a combination of standard and specialized software. Data was digitized using VACUUM MkI (M.B.C. Systems, Mt. Washington Station, Baltimore, MD, U.S.A.) software and Data Translation (Marlborough, MA, U.S.A.) hardware (DT 2805). Current records were fitted by a non-linear least-squares method using a modified Marquardt algorithm (MARQFIT.BAS; Schreiner, Kramer, Krischer & Langman (1985) with modifications by N. M. Cohen) to a single exponential equation:

$$I(t) = \{A[\exp(-t/\tau)] + \text{offset}\}. \quad (1)$$

The amplitude (A) of I_{Ca} was estimated at $t = 0$ and the time constant of decay by the time variable (τ). We have used four methods of assessing the amplitude of I_{Ca} : (1) non-linear least-squares fit of a single exponential (see above) which yields a residual current (the difference between the estimated current and the recorded current) due to the non-exponentiality of the recorded current that is both inward and outward; (2) best fit of a single exponential such that the residual current is inward; (3) best fit of a single exponential such that the residual current is outward; and (4) peak I_{Ca} recorded. As expected, the estimated time constants are different using the four methods as shown in Fig. 2B. These differences are small and the voltage dependence of τ is virtually unchanged. We suspect that the non-exponentiality of I_{Ca} is dependent on I_{Ca} , or some consequence of it, since the calcium channel blocker D600 removes both the exponential current and the residual current (see Fig. 6). Since calcium-activated inward currents have been reported in this preparation (Colquhoun, Neher, Reuter & Stevens, 1981) and since calcium-activated outward currents are seen generally in heart muscle (e.g. Kass & Tsien, 1975, 1976; Siegelbaum & Tsien, 1980), both may contaminate our measured currents. In order to determine how much d_{∞} and f_{∞} depend on our method of estimating the magnitude of I_{Ca} , we determined d_{∞} and f_{∞} using all four methods to estimate I_{Ca} . We found that each method gave essentially the same results as shown in Fig. 4. In the analysis in this paper we chose to use method (1), a result generated by the least-squares fit described above, because we believe there may well be both calcium-activated inward and outward currents in this preparation.

The data for the steady-state kinetic parameters were fitted to the following Boltzmann equations:

$$d_{\infty} = [1 + \exp(-(V - V_h)/k)]^{-1}, \quad (2)$$

$$f_{\infty} = [1 + \exp((V - V_h)/k)]^{-1}, \quad (3)$$

where V is the membrane potential, V_h and k are constants.

RESULTS

Action potentials

Action potentials recorded from a cultured neonatal rat heart cell are shown in Fig. 1. The control record shows an action potential similar in shape to action potentials previously described (Langer, Brady, Tan & Serena, 1975; Jourdan, 1984). The calcium channel antagonist D600 depresses the plateau of the action potential while the calcium channel agonist BAY K8644 prolongs it. Since I_{Ca} inactivates rapidly at plateau potentials (Isenberg & Klockner, 1982) alteration of only the transient component of I_{Ca} is unlikely to fully account for the effects of these agents. This suggests that an investigation of the steady-state component of I_{Ca} may be useful. A steady-state component of the sodium current has been identified in cardiac

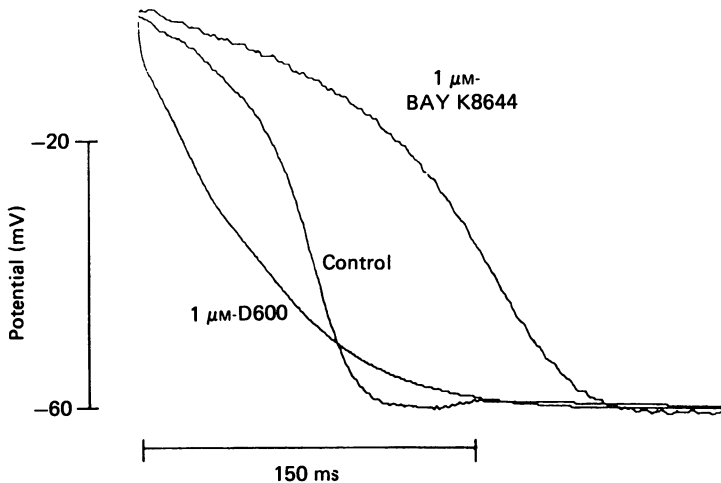


Fig. 1. Action potential records from neonatal rat cardiac myocytes. Action potentials were recorded from single cultured cells after a 1 ms stimulus under control conditions, after 5 min exposure to $1 \mu\text{M}$ -BAY K8644 and after 5 min exposure to $1 \mu\text{M}$ -D600. Similar effects of D600 on the action potential were observed following the addition of $1 \mu\text{M}$ -D600 alone.

Purkinje fibres ('window current'; Attwell *et al.* 1979) and shown to be important in modulating action potential duration (Colatsky, 1982) and thereby affecting arrhythmogenic currents (Sheu & Lederer, 1985). We were particularly interested in determining whether a similar steady-state calcium channel 'window current' exists in ventricular myocytes and the mechanism by which it may be modulated.

*Calcium current (I_{Ca})**General*

Calcium channel currents were recorded under control conditions with Ca^{2+} as the principal current carrier. In order to examine only the role of 'L' type calcium channels in 'whole-cell' current records, the holding potential was set to -50 mV (Nilius *et al.* 1985). If any 'T' type channels were present in this preparation, they would be inactivated by this holding potential. Depolarizing pulses of 200 ms duration to potentials between -50 and $+60 \text{ mV}$ were applied at 0.5 Hz. We noted

four features of I_{Ca} (see Fig. 2): (1) following activation and inactivation a steady-state current was observed; (2) the magnitude of the inward current transient and the steady-state current increased with depolarizations between -40 and 0 mV and decreased between $+5$ and $+50$ mV; (3) the time-dependent component reversed direction at $+55$ mV; (4) over the voltage range 0 to $+55$ mV the rate of inactivation decreased with increasing depolarization. To examine I_{Ca} over a wider voltage range, the data shown in Fig. 2B and C was obtained by stepping the membrane potential briefly (10 ms) to -90 mV and then to various test potentials (V_{test}) for 200 ms once every 2 s. Over the test potential range of -80 to -40 mV no phasic current was recorded. V_{test} over the range of -40 to 0 mV led to an increasing I_{Ca} transient with greater depolarization but the inactivation time constants (τ) were relatively constant at about 10 ms. Over the range of V_{test} from $+5$ to $+60$ mV the magnitude of the I_{Ca} transient decreased but τ increased from 10 ms to about 75 ms. The transient component of I_{Ca} reversed direction at about $+55$ mV, becoming an outward current at more positive potentials, a value similar to that reported by Lee & Tsien (1982).

Steady-state current-voltage relationship

Fig. 3 shows the current-voltage relationship measured at the end of 200 ms voltage-clamp pulses. A 10 ms pre-pulse to -90 mV was applied from the holding potential of -50 mV and was followed by a 200 ms test pulse; this protocol was repeated at 0.5 Hz. To block outward potassium channels 20 mM-CsCl was added to the pipette solution and the resulting current-voltage relationship is shown (Δ). Additionally, sodium channels were blocked by adding $10 \mu\text{M}$ -TTX to the superfusion solution (\diamond). Separate experiments (not shown) indicate that no further sodium channel blockade was achieved by increases in TTX concentration up to $20 \mu\text{M}$. The TTX-sensitive current shown in Fig. 3B suggests the existence of a sodium channel 'window current' in neonatal cells that is analogous to that reported in cardiac Purkinje fibres (Attwell *et al.* 1979; Colatsky, 1982). D600 was then added to block I_{Ca} (\blacksquare). The difference between the current records in the presence (\blacksquare) and absence (\diamond) of D600 is the D600-sensitive current shown in Fig. 3C. This presumably represents the steady-state I_{Ca} , the calcium channel 'window current' (see also Fig. 4D). There is still a small component of steady-state inward current in the caesium-loaded, TTX- and D600-superfused cells which may reflect a component of TTX-insensitive sodium current and/or a D600-insensitive calcium current. This contamination is not large (less than 4% of the I_{Ca} peak). Additionally there is a similarly small component of outward current at potentials positive to $+55$ mV that may reflect the same thing. Another possible explanation is that the small steady-state current is due to the voltage dependence of the sodium-pump current (Gadsby, Kimura & Noma, 1985) and the sodium-calcium exchange current (Kimura, Noma & Irisawa, 1986).

Steady-state I_{Ca} variables (d_{∞} and f_{∞})

To investigate the steady-state I_{Ca} observed in Fig. 3 we measured steady-state activation (d_{∞}) and steady-state inactivation (f_{∞}) variables and the results are displayed in Fig. 4.

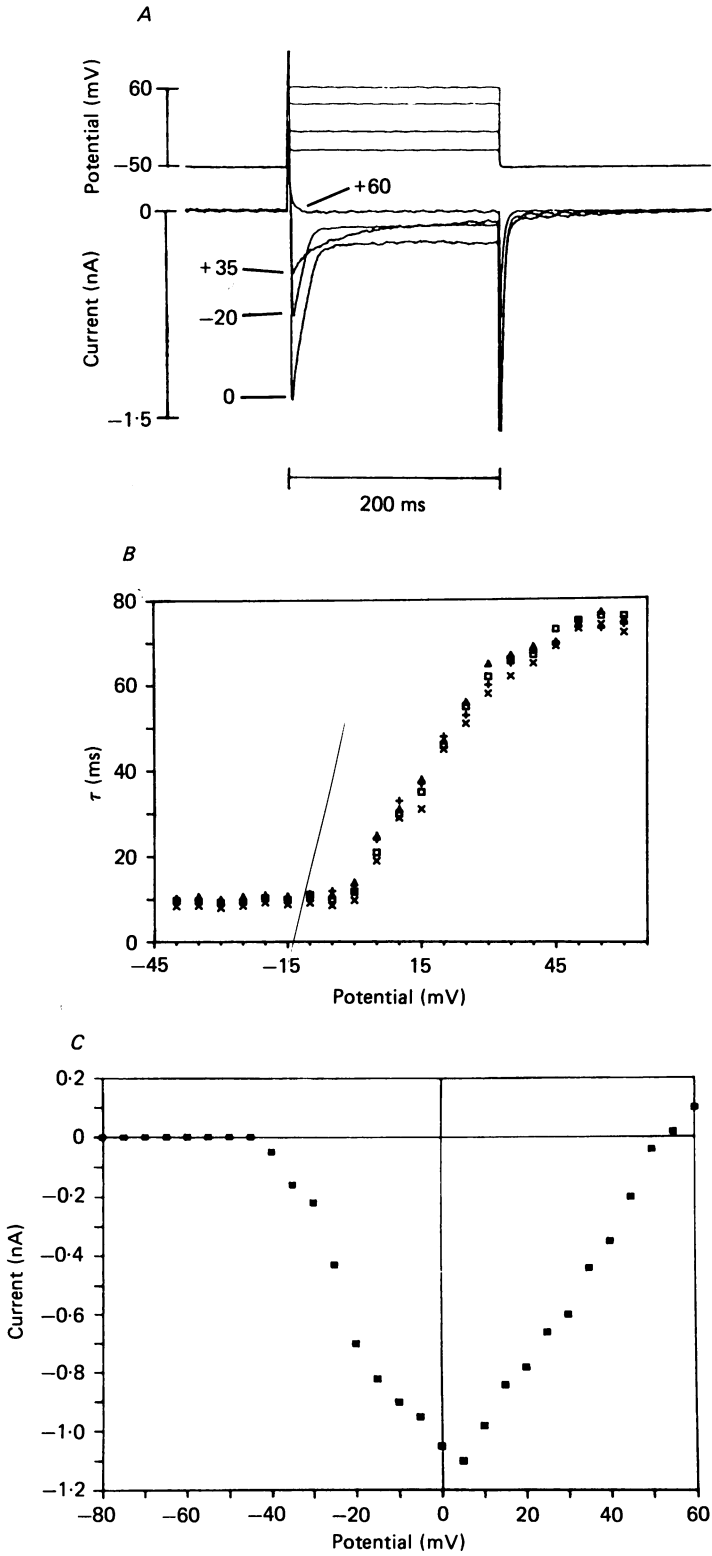


Fig. 2. For legend see opposite.

To investigate d_∞ , the membrane potential was held at -50 mV. A 10 ms pre-pulse to -90 mV was followed by a 10 ms pulse to V_{test} . The tail current (I_{test}) was measured on returning to the holding potential following V_{test} . In order to control for I_{Ca} 'run-down' (Byerly & Hagiwara, 1982; Fenwick, Marty & Neher, 1982; Bean, 1984; Lee & Tsien, 1984), all trials to V_{test} were alternated with trials to $V_{\text{test}}^{\text{max}}$ (the test potential that gives the largest tail current) and the ratio of the resulting tail currents ($I_{\text{test}}/I_{\text{test}}^{\text{max}}$) was determined and plotted in Fig. 4A. The smooth curve shows the best-fit line described by a Boltzmann equation ($V_h = -3.2$ mV, $k = 6.72$ mV).

To investigate f_∞ the membrane potential was held at -50 mV. Following a 200 ms voltage-clamp step to V_{test} , the membrane potential was hyperpolarized to -90 mV for 10 ms, and then depolarized to the evaluation potential ($+5$ mV) for 200 ms before returning to the holding potential. To control for I_{Ca} 'run-down' all trials to V_{test} were alternated with trials to $V_{\text{test}}^{\text{max}}$ (the test potential that gives the largest current transient at the evaluation potential) and the ratio of the resulting currents ($I_{\text{test}}/I_{\text{test}}^{\text{max}}$) was plotted in Fig. 4B. The smooth curve shows the best-fit line described by a Boltzmann equation ($V_h = -7.0$ mV, $k = 9.31$ mV).

In Fig. 4C we have plotted both d_∞ and f_∞ . These results show a large overlap of the two curves (hatched area). The voltage dependence of the overlap of d_∞ and f_∞ constitutes a voltage range where significant steady-state I_{Ca} should be seen. Fig. 4D shows a plot of the predicted shape of the steady-state calcium-current-voltage relationship (continuous line, see below). Note that the voltage dependence of the steady-state I_{Ca} is generally similar to that of the D600-sensitive current shown in Fig. 3C. The small outward current at potentials positive to $+55$ mV in Fig. 3C, which is also shown in Fig. 4D (where $d_\infty \times f_\infty$ is zero) may be due to a D600-sensitive potassium current (Kass & Tsien, 1975; Hume, 1985). This small current would contribute proportionally less contaminating current as the membrane potential approached the potassium reversal potential.

Timing of voltage protocols to measure d_∞ and f_∞

With depolarization, activation of I_{Ca} occurs much more rapidly than inactivation of I_{Ca} (see e.g. Sanguinetti *et al.* 1986). Our measurement of d_∞ makes use of the voltage protocol described in Fig. 4A. In order to optimize the measurement of I_{test} , V_{test} must be maintained for a sufficiently long duration to attain activation without producing excessive inactivation. In Fig. 5A we show d_∞ for different durations of V_{test} . When the duration of V_{test} is between 5 and 20 ms, the values of V_h and k are

Fig. 2. Calcium current (I_{Ca}) from neonatal rat cardiac myocytes. A, records of potential and current elicited by depolarizing pulses for 200 ms to potentials of -20 , 0 , $+35$ and $+60$ mV from the holding potential of -50 mV are shown. In B and C, the membrane potential was stepped to -90 mV for 10 ms and then to various test potentials for 200 ms once every 2 s. The time constant of decay (τ) of the I_{Ca} transient (B) and the magnitude of the I_{Ca} transient (C) are shown as a function of potential. In B, the time constants used to fit the current records employing the different fitting methods are plotted at each potential (see Methods). \square , least-squares fit; \times , inward residual current; \triangle , outward residual current; $+$, time of decay to $1/e$ of peak I_{Ca} recorded (no curve fitting).

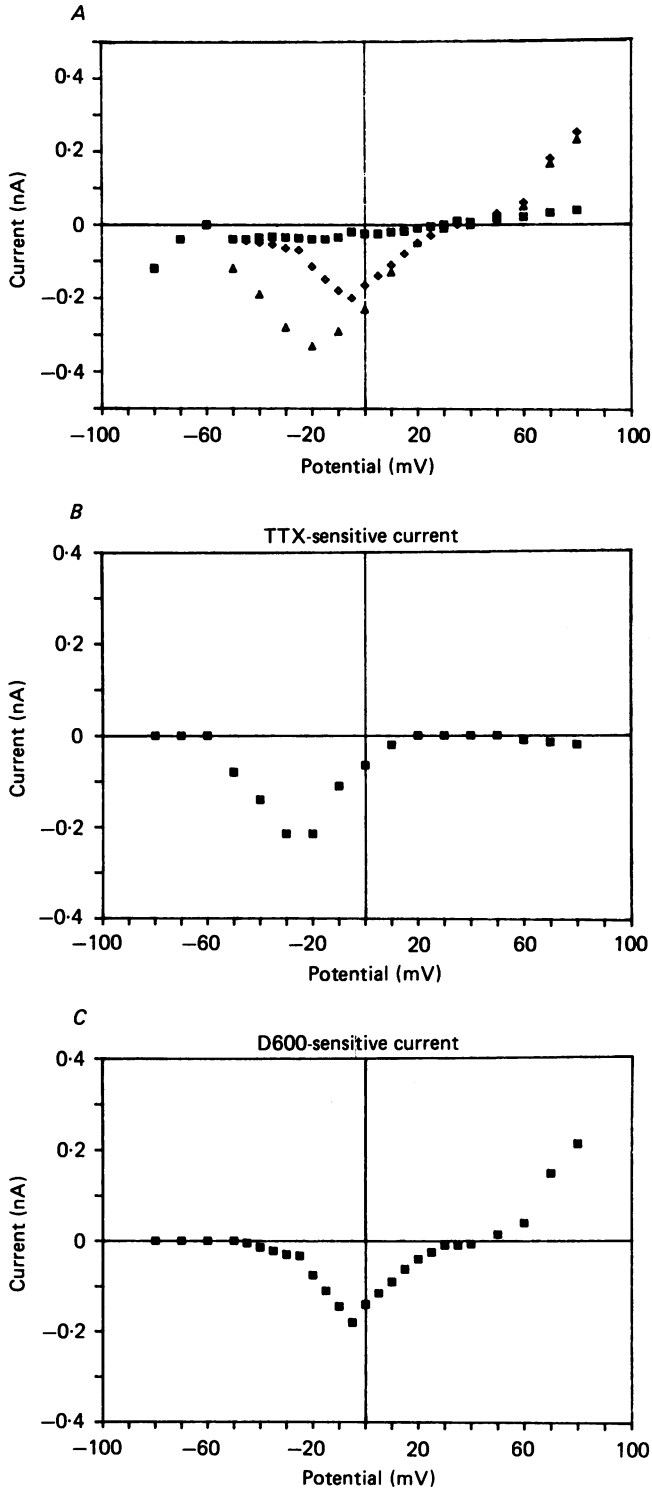


Fig. 3. For legend see opposite.

similar, with the largest maximum I_{test} being achieved at 10 ms. If however, the test-pulse duration is lengthened to 50 ms, the effects of inactivation are large.

When measuring f_{∞} it is important that the pre-pulse duration (V_{test}) is sufficiently long to allow inactivation to reach a steady-state condition (see Fig. 4B for protocol). Fig. 5B shows the effect of pre-pulse duration on the $I_{\text{test}}/I_{\text{test}}^{\text{max}}$ ratio. While a V_{test} duration of 100 ms is insufficient, steady-state inactivation is attained when the pre-pulse duration is lengthened to 200 ms. A further increase of V_{test} duration to 500 ms does not affect the measurement of f_{∞} . We consequently chose to use a V_{test} duration of 200 ms.

The effect of D600 on I_{Ca}

General

Fig. 6A shows records of I_{Ca} recorded in response to 200 ms depolarizing pulses to +5 mV from -50 mV applied at 0.5 Hz (to avoid rate-dependent effects of D600; McDonald, Pelzer & Trautwein, 1980). D600 decreases the magnitude of both the steady-state and transient components of I_{Ca} in a dose-dependent manner, with 1 μM -D600 completely abolishing both components of I_{Ca} . Fig. 6B shows the voltage dependence of the inactivation time constant which is not significantly affected by D600. The shape of the transient component of calcium-current-voltage relationship is not significantly changed with increasing doses of D600 (Fig. 6C), but the peak of the relationship is decreased and shifted to more positive potentials. Fig. 6D shows how the voltage dependence of the steady-state component of I_{Ca} changes with increasing D600 concentration. The changes in the steady-state component of I_{Ca} are very similar to those seen for the transient component of I_{Ca} .

The effect of D600 on d_{∞} and f_{∞}

To measure the effect of D600 on d_{∞} and f_{∞} we used the same protocols described in Fig. 4. D600 produces a dose-dependent shift of d_{∞} to more positive potentials as shown in Fig. 7A. D600 increases V_{h} without materially affecting k (see Table 1). D600 has only a small effect on f_{∞} as shown in Fig. 7B. These results are in agreement with earlier examinations of I_{Ca} and D600 (McDonald *et al.* 1984). The effect of D600 on both d_{∞} and f_{∞} is shown in Fig. 7C. D600 leads to a decrease in the magnitude of the overlap of d_{∞} and f_{∞} and the overlap shifts to more positive potentials. We have calculated the anticipated shape of the transient component of I_{Ca} ($I_{\text{Ca}}^{\text{tr}}$), assuming that the kinetics of activation are always much faster than the kinetics of

Fig. 3. Steady-state current-voltage relationships. *A*, a 10 ms pre-pulse to -90 mV was applied from the holding potential of -50 mV and was followed by a 200 ms test pulse. The magnitude of the current remaining at the end of the test pulse is plotted as a function of voltage. Caesium was included in the pipette solution (Δ) to block potassium channels. Subsequently, 10 μM -TTX was added to the superfusion solution (\diamond) to block sodium channels. 1 μM -D600 was then further added to the superfusion solution (\blacksquare) to block calcium channels. *B*, TTX-sensitive steady-state current. The difference between (\diamond) and (Δ) in *A* is plotted as a function of potential. *C*, D600-sensitive steady-state current. The difference between (\blacksquare) and (\diamond) in *A* is plotted as a function of potential.

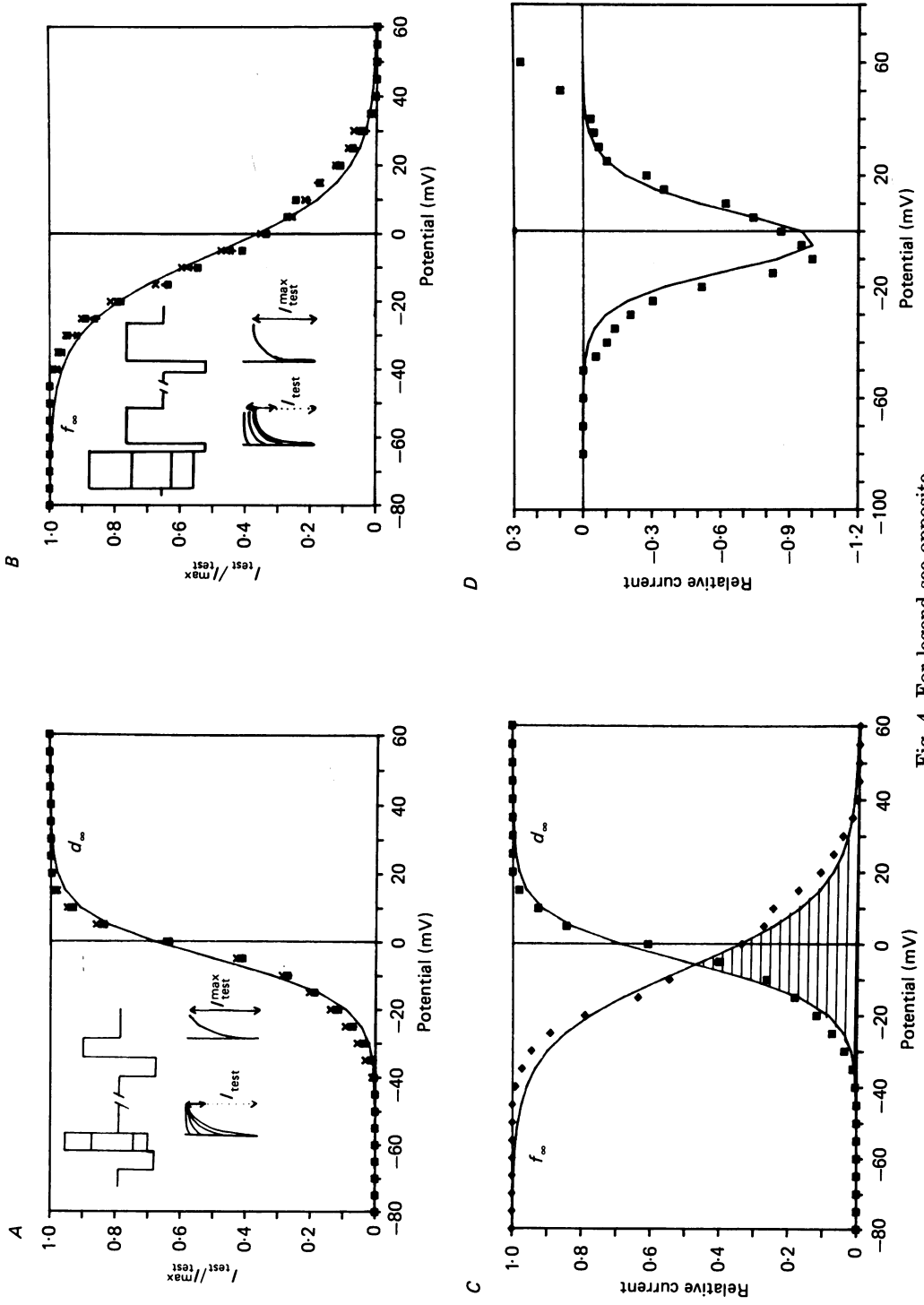


Fig. 4. For legend see opposite.

TABLE 1. The effects of D600 on parameters of I_{Ca}

	D600			D600			
	Control	50 nM	100 nM	Control	50 nM	100 nM	
		d_{∞}			f_{∞}		
V_h (mV)	-3.0 ± 1.6	6.9 ± 2.2	25.2 ± 4.8	-6.9 ± 1.5	-7.0 ± 3.4	-2.1 ± 3.8	
k (mV)	6.7 ± 0.18	6.6 ± 0.21	6.6 ± 0.27	9.4 ± 0.35	9.4 ± 0.32	9.6 ± 0.3	
		Transient I_{Ca}			Steady-state I_{Ca}		
g_r (nS)	25.2 ± 4	19.8 ± 7	15.8 ± 9	24.2 ± 5	23.8 ± 7	21.2 ± 7	
n	10	5	5	10	5	5	

inactivation. The calculation also uses a voltage-independent ‘relative conductance’ variable, g_r ,

$$I_{Ca}^{tr}(V_m) = g_r(V_m - E_{ch}) d_{\infty}(V_m) [1 - f_{\infty}(V_m)], \tag{4}$$

where V_m is the membrane potential and E_{ch} is the channel reversal potential. The smooth curves generated by eqn. (4), which make use of the relevant $d_{\infty}(V_m)$ and $f_{\infty}(V_m)$ curves, and an adjusted g_r are shown in Fig. 6C. The smooth curves of Fig. 6C fit the data points fairly well. The deviations have been seen consistently and could reflect some voltage dependence of the g_r function. An additional explanation is the possible slowing of the activation kinetics relative to the inactivation kinetics at more positive potentials. We have no direct evidence regarding either explanation (see Discussion).

Fig. 4. Steady-state activation (d_{∞}) and inactivation (f_{∞}) variables. *A*, steady-state activation (d_{∞}) as a function of potential. The tail current following a test potential (I_{test}) is measured as is the maximum tail current (I_{test}^{max}). The magnitude of the tail current was determined by four different methods (see Methods): ■, non-linear least-squares fit; (x) residual inward current; ▲, residual outward current; +, peak I_{Ca} recorded (no curve fitting). The ratio I_{test}/I_{test}^{max} is plotted as a function of V_{test} and is unaffected by the method of estimating the tail current magnitude. The smooth curve is the best fit of the data to a Boltzmann equation (see Methods). *B*, steady-state inactivation (f_{∞}) as a function of potential. The current elicited by a standard depolarization to 5 mV following a pre-pulse to a test potential for 200 ms (I_{test}) is measured, as is the current recorded on depolarization to 5 mV from the holding potential of -50 mV with no pre-pulse (I_{test}^{max}). The magnitude of the current was determined by four different methods (see Methods): ■, non-linear least-squares fit; x, residual inward current; ▲, residual outward current; +, peak I_{Ca} recorded (no curve fitting). The ratio I_{test}/I_{test}^{max} is plotted as a function of V_{test} and is unaffected by the method of estimating the current magnitude. The smooth curve is the best fit of the data to a Boltzmann equation. *C*, overlap of d_{∞} and f_{∞} . The curves showing the voltage dependence of d_{∞} and f_{∞} from *A* and *B* are plotted together. The overlap of d_{∞} and f_{∞} (hatched area) represents a voltage range over which both d_{∞} and f_{∞} are non-zero and steady-state calcium current (‘window current’) will flow. *D*, the steady-state current-voltage relationship of I_{Ca} . Assuming that the relative conductance ($g_r = 23.21$ nS) is not a function of voltage and the reversal potential for I_{Ca} is +55 mV, the continuous line is the calculated steady-state I_{Ca} from *C* and the equation:

$$I_{Ca}^{ss} = g_r(V_m - 0.055) d_{\infty}(V_m) f_{\infty}(V_m).$$

The data points are taken from Fig. 3C with appropriate scaling.

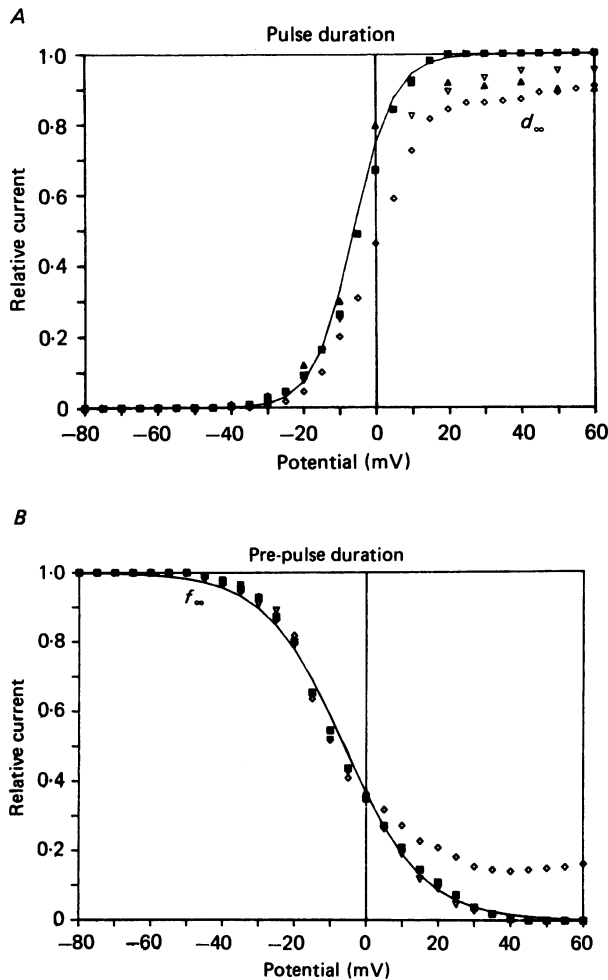


Fig. 5. Timing of voltage protocols to measure d_{∞} and f_{∞} . *A*, effect of altering test pulse duration on d_{∞} . The experimental protocol was identical to that used in Fig. 4*A* except that the V_{test} was: ∇ , 5 ms; \blacksquare , 10 ms; \blacktriangle , 20 ms; or \diamond , 50 ms, and that $V_{\text{test}}^{\text{max}}$ duration was fixed at 10 ms. *B*, effect of altering pre-pulse duration on f_{∞} . The experimental protocol was identical to that shown in Fig. 4*B* except that the V_{test} duration was: \diamond , 100 ms; \blacksquare , 200 ms; or ∇ , 500 ms, and the $V_{\text{test}}^{\text{max}}$ duration was fixed at 200 ms.

Fig. 6. The effect of D600 on I_{Ca} . *A*, original records of current and voltage. Currents were elicited by depolarizing steps to +5 mV from the holding potential (-50 mV) for 200 ms in the presence of increasing concentrations of D600. *B*, the effect of D600 on the time constant of decay (τ) of I_{Ca} . \blacksquare , control; \blacklozenge , 50 nM-D600; \blacktriangledown , 100 nM-D600. *C*, the effect of D600 on the transient component of the calcium-current-voltage relationship. The smooth curves are predicted from the measured d_{∞} and f_{∞} (see Fig. 7) and eqn. (4). \blacksquare , control ($g_r = 24.39$ nS); \blacklozenge , 50 nM-D600 ($g_r = 19.61$ nS); \blacktriangledown , 100 nM-D600 ($g_r = 15.38$ nS); $+$, 1 μM -D600. $E_{\text{ch}} = +53$ mV. *D*, the effect of D600 on the current-voltage relationship of the steady-state component of I_{Ca} . The smooth curves are predicted from the measured d_{∞} and f_{∞} (see Fig. 7) and eqn. (5). \blacksquare , control ($g_r = 22.22$ nS); \blacklozenge , 50 nM-D600 ($g_r = 23.81$ nS); \blacktriangledown , 100 nM-D600 ($g_r = 22.22$ nS). $E_{\text{ch}} = +53$ mV.

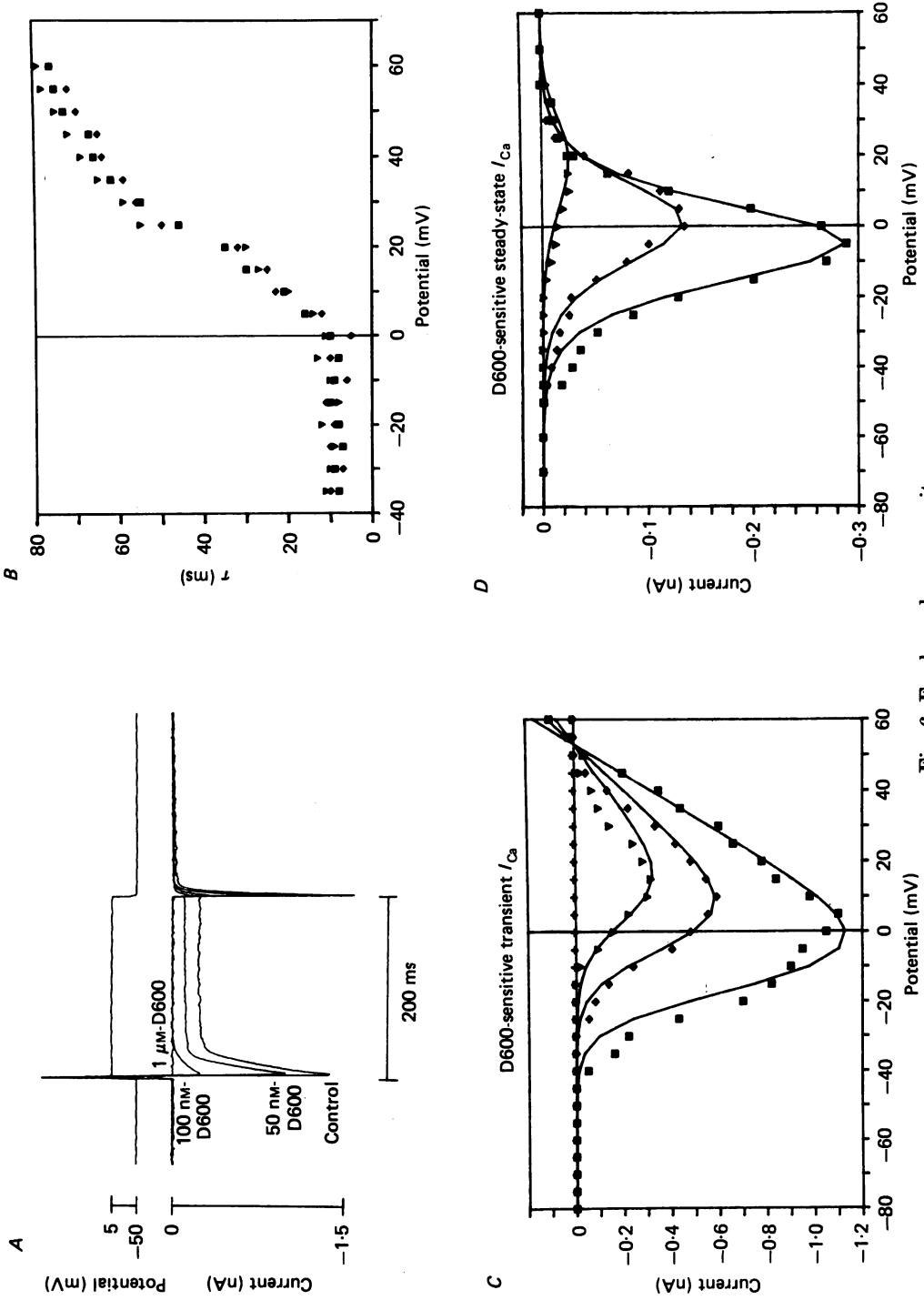


Fig. 6. For legend see opposite.

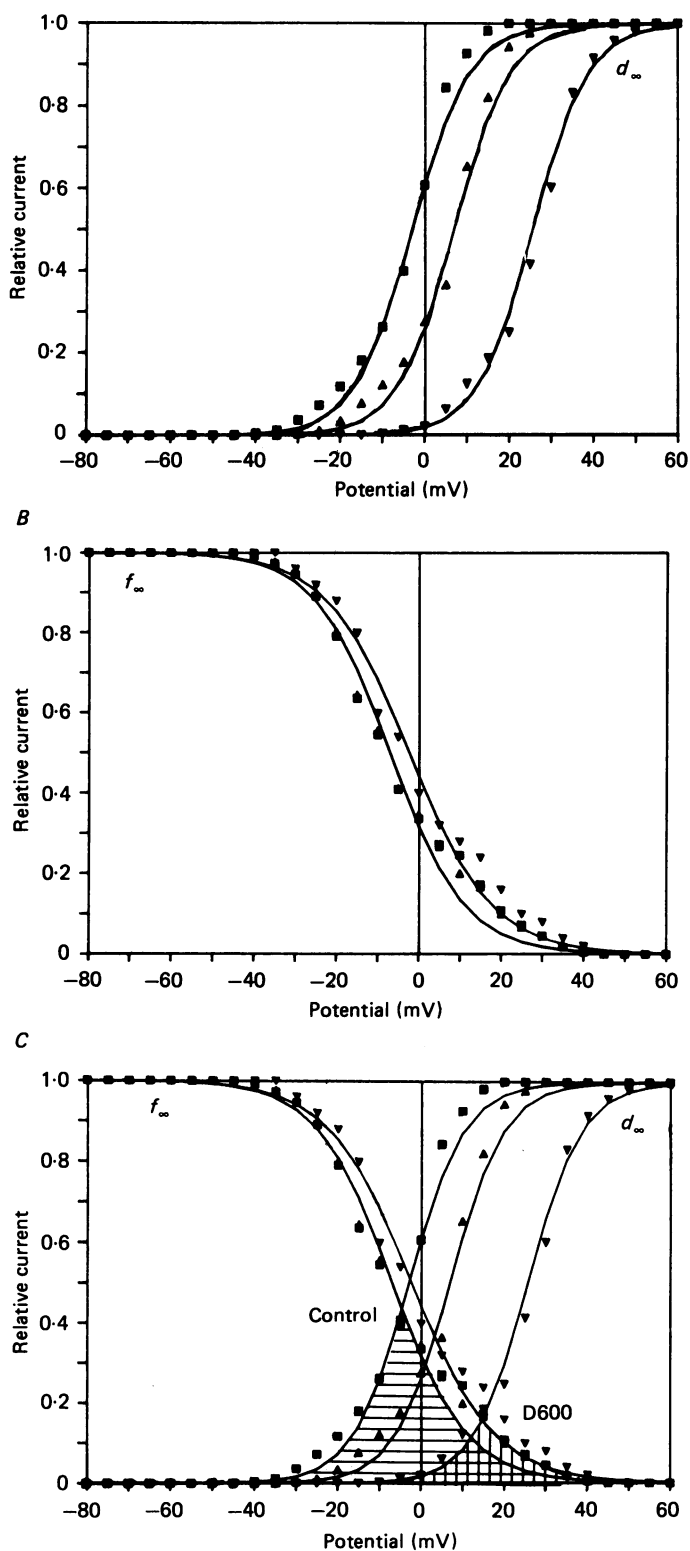


Fig. 7. For legend see opposite.

The d_∞ and f_∞ curves can also be used to predict the steady-state component of I_{Ca} (I_{Ca}^{SS}). The major assumption is that the 'relative conductance' variable, g_r , is voltage independent.

$$I_{Ca}^{SS}(V_m) = g_r(V_m - E_{ch}) d_\infty(V_m) f_\infty(V_m). \quad (5)$$

The smooth curves shown in Fig. 6D fit the experimental data well.

The results summarized in Table 1 indicate that the g_r values used to fit the transient and steady-state calcium-current-voltage relationships to I_{Ca} experimental results are similar. Additionally, g_r decreases with increasing D600 concentration. Presumably $g_r = W\gamma_{ch}n$, where W is a probability weighting coefficient reflecting the probability that the channel is open independent of d_∞ and f_∞ , γ_{ch} is the single-channel conductance and n is the number of functional channels. The decrease in g_r that we observe cannot be attributed to a decrease in γ_{ch} since D600 has been shown not to alter γ_{ch} (Cavalié *et al.* 1985). Possible physical interpretations of W are presented in the Discussion. The reduction in both steady-state and transient components of I_{Ca} in the presence of D600 thus reflects both alteration in g_r as well as in d_∞ .

The effect of BAY K8644 on I_{Ca}

General

Fig. 8A shows records of current and voltage at various test potentials in the presence and absence of $1 \mu\text{M}$ -BAY K8644. From the holding potential of -50 mV (a potential at which BAY K8644 acts as a calcium channel agonist; Sanguinetti & Kass, 1984*a, b*; Sanguinetti *et al.* 1986) the membrane potential was depolarized to various test potentials for 200 ms once every 2 s to avoid rate-dependent effects on the dihydropyridine action (Sanguinetti & Kass, 1984*a*). Both transient and steady-state components of I_{Ca} were affected by BAY K8644 as shown in Fig. 8. The inactivation time constant was decreased at positive potentials in the presence of BAY K8644 (Fig. 8B). There was a voltage-dependent increase in the magnitude of the transient component of I_{Ca} produced by the addition of BAY K8644 (Fig. 8C). Over the voltage range -80 to -40 mV no transient component of I_{Ca} was recorded, a finding similar to that seen in the absence of BAY K8644. From -40 to $+5 \text{ mV}$ the magnitude of the transient component of I_{Ca} was greater in the presence of BAY K8644 than in its absence while the time constant of inactivation was relatively unaffected. From $+20$ to $+60 \text{ mV}$ the magnitude of the transient component of I_{Ca} was nearly the same in the presence and absence of BAY K8644 but the time constant of inactivation was less. In the presence of BAY K8644 the magnitude and the shape of the transient component of calcium-current-voltage relationship was changed and

Fig. 7. The effect of D600 on the steady-state activation (d_∞) and inactivation (f_∞) variables. *A*, the effect of D600 on steady-state activation (d_∞). ■, control ($V_h = -3.5 \text{ mV}$, $k = 6.55 \text{ mV}$); ▲, 50 nM-D600 ($V_h = 6.5 \text{ mV}$, $k = 6.5 \text{ mV}$); ▼, 100 nM-D600 ($V_h = 25.6 \text{ mV}$, $k = 6.48 \text{ mV}$), *B*, the effect of D600 on steady-state inactivation (f_∞). ■, control ($V_h = -6.85 \text{ mV}$, $k = 9.05 \text{ mV}$); ▲, 50 nM-D600 ($V_h = -6.96 \text{ mV}$, $k = 9.03 \text{ mV}$); ▼, 100 nM-D600 ($V_h = -1.7 \text{ mV}$, $k = 9.86 \text{ mV}$). *C*, the effect of D600 on the overlap of d_∞ and f_∞ .

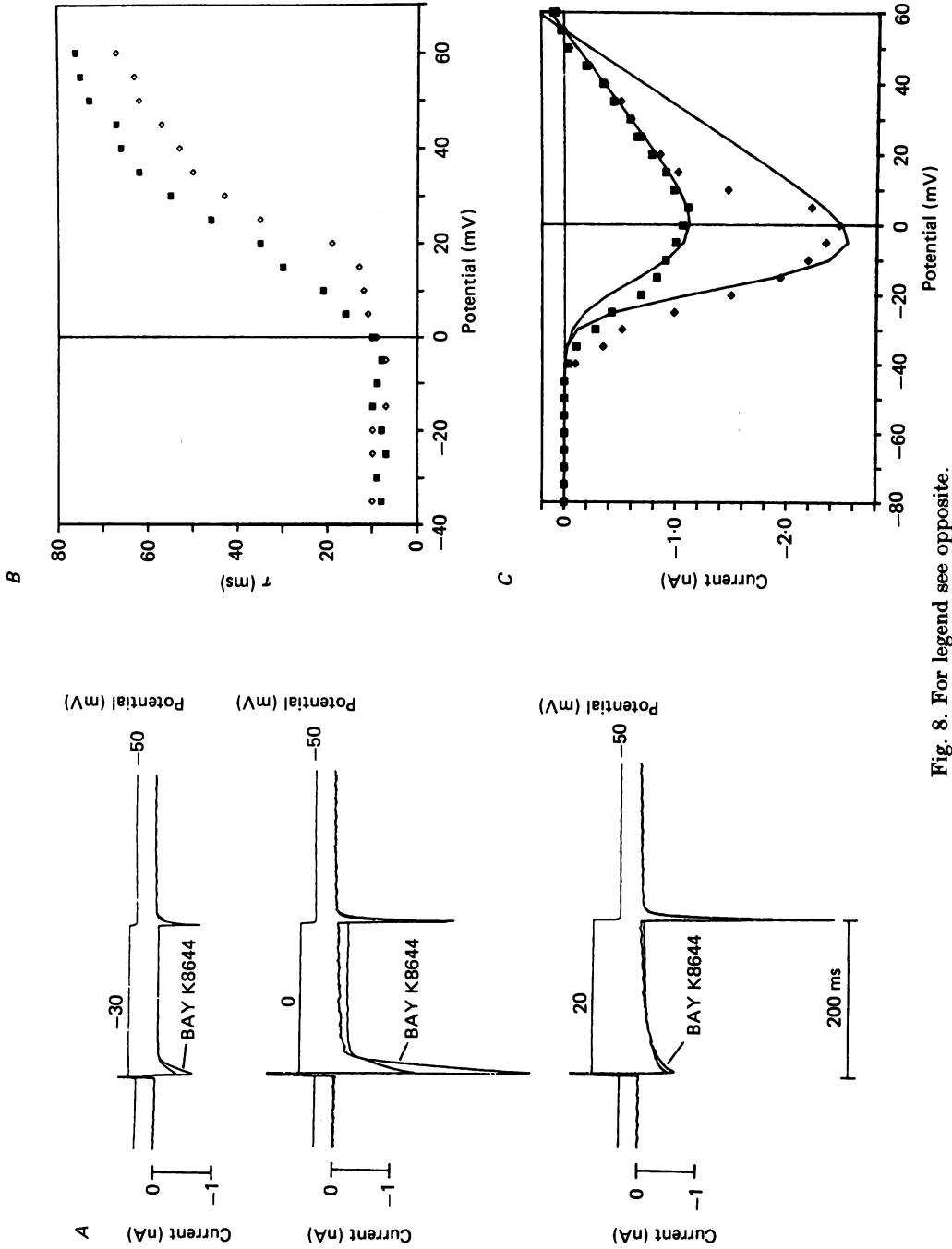


Fig. 8. For legend see opposite.

TABLE 2. The effects of BAY K8644 on parameters of I_{Ca}

	d_{∞}		f_{∞}	
	Control	1 μ M-BAY K8644	Control	1 μ M-BAY K8644
V_h (mV)	-3.0 \pm 1.6	-14.2 \pm 2.4	-6.9 \pm 2.5	-18.6 \pm 3.5
k (mV)	6.7 \pm 0.18	6.22 \pm 0.42	9.4 \pm 0.35	5.1 \pm 0.28
Transient I_{Ca}				
g_r (nS)	25.2 \pm 4	54.3 \pm 11		
n	10	5	10	5

the peak was shifted 5 mV in the hyperpolarizing direction (Fig. 8C) consistent with the results of others (Sanguinetti *et al.* 1986).

The effect of BAY K8644 on d_{∞} and f_{∞}

The effects of BAY K8644 on d_{∞} and f_{∞} are shown in Fig. 9. The voltage protocols used to measure d_{∞} and f_{∞} were the same as those described in Fig. 4. BAY K8644 had marked effects both on d_{∞} (Fig. 9A) and on f_{∞} (Fig. 9B). d_{∞} was shifted in the hyperpolarizing direction but with relatively little effect on k (Table 2). f_{∞} was also shifted in the hyperpolarizing direction. Unlike other results presented, BAY K8644 increased the slope of the f_{∞} curve (see value of k , Table 2). The effect of these changes in d_{∞} and f_{∞} on the overlap of these two parameters is shown in Fig. 9C. The magnitude of the overlap of d_{∞} and f_{∞} was unchanged but the voltage range of the overlap was shifted in the hyperpolarizing direction by about 15 mV.

Using the d_{∞} and f_{∞} curves that we measured, we have attempted to fit the measured values of the transient component of I_{Ca} as we did for D600. The results using eqn. (4) and the relevant $d_{\infty}(V_m)$ and $f_{\infty}(V_m)$ curves (Fig. 9C) are shown as the smooth curves in Fig. 8C. At positive potentials the prediction of transient I_{Ca} magnitude deviates from the experimental results. This may be due to a voltage dependence of g_r or relative slowing of the activation kinetics *versus* the inactivation kinetics. Although we have no direct evidence about the effect BAY K8644 will have on activation kinetics, we do observe an increased rate of inactivation at these potentials (Fig. 8B).

DISCUSSION

We have described the characteristics of 'L' type 'whole-cell' calcium channel current (I_{Ca}) in single cells of the neonatal rat heart. The current that we record is comprised of two components – a transient component and a steady-state component (Figs. 2 and 3). The current–voltage relationship of the transient component is similar

Fig. 8. The effect of BAY K8644 (1 μ M) on I_{Ca} . *A*, original records of current and voltage. Current records were recorded in response to 200 ms depolarizing voltage steps to -30, 0 and +20 mV in the presence and absence of 1 μ M-BAY K8644. *B*, the effect of BAY K8644 on the time constant of inactivation (τ) of I_{Ca} . ■, control; ◇, BAY K8644. *C*, the effect of BAY K8644 on the transient component of calcium-current–voltage relationship. The smooth curves are predicted from the measured d_{∞} and f_{∞} curves (see Fig. 9) and eqn. (4). ■, control ($g_r = 23.81$ nS); ◆, 1 μ M-BAY K8644 ($g_r = 47.62$ nS).

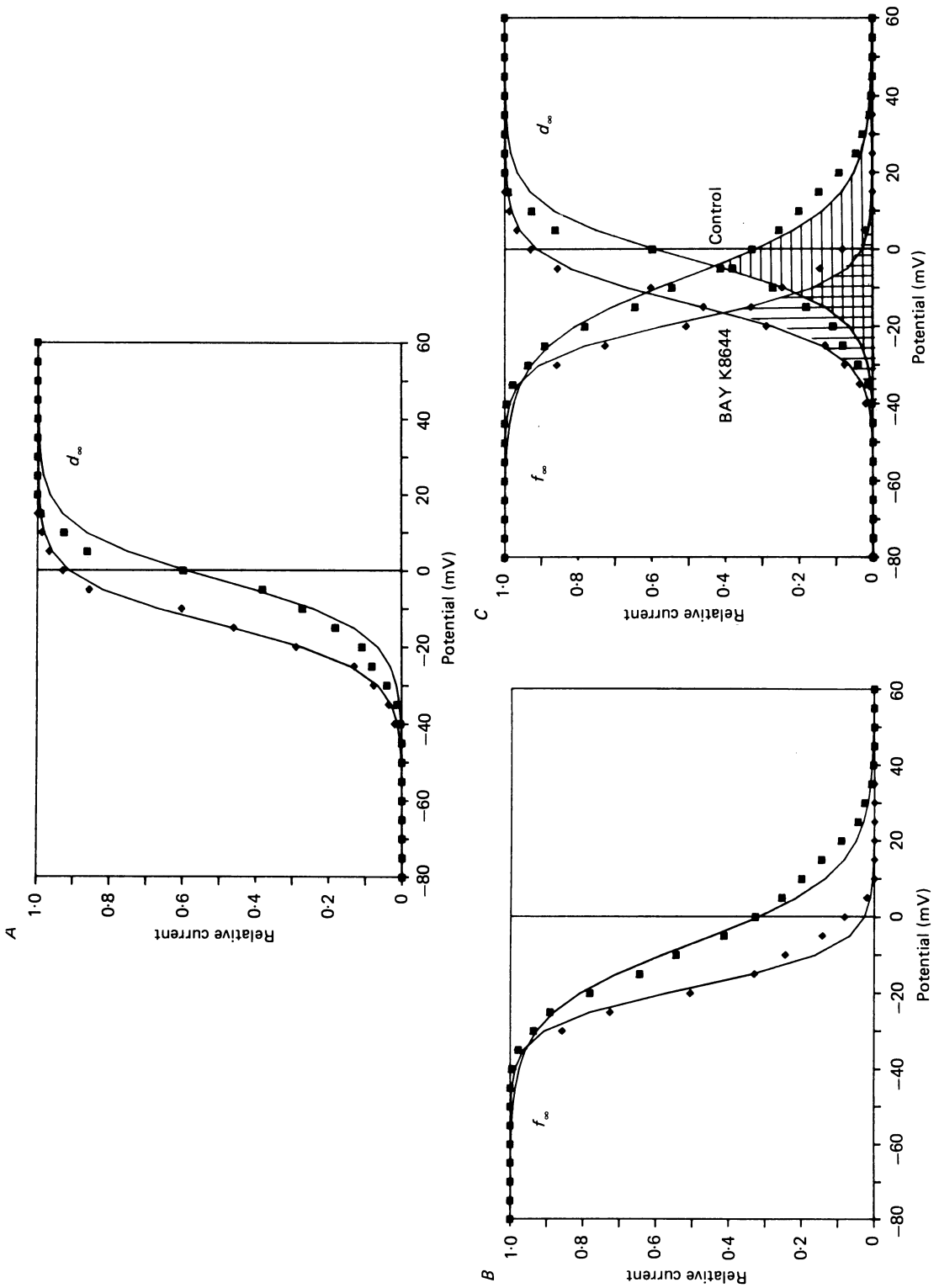


Fig. 9. For legend see opposite.

to that of I_{Ca} reported in other cardiac cells (Isenberg & Klockner, 1982; Mitchell *et al.* 1983; Hess *et al.* 1984; Bean, 1985). The voltage dependence of the time constant of inactivation (τ) is sigmoid in contrast to the U-shaped relationship described in other cells (Isenberg & Klockner, 1982; Nilius & Roeder, 1985). We have measured the steady-state activation (d_∞) and inactivation (f_∞) variables and they are well described by Boltzmann equations (Fig. 4). The voltage dependence of the overlap d_∞ and f_∞ ('window current') is similar to the voltage dependence of the measured steady-state I_{Ca} (Fig. 3). Furthermore, the current-voltage relationship of the steady-state component of I_{Ca} can be predicted from considerations of the relative conductance (g_r), the driving force ($V_m - E_{ch}$), and the d_∞ and f_∞ curves (cf. eqn. (5) and Fig. 4).

We have examined the effects of the calcium channel antagonist D600 on I_{Ca} . We find that D600 blocks both components of I_{Ca} in a dose-dependent manner with $1 \mu\text{M}$ -D600 abolishing I_{Ca} fully (Fig. 6). D600 shifts d_∞ to more positive potentials without any significant effects on f_∞ . The net result of the shift in d_∞ is to decrease the magnitude of the 'window current' and shift its voltage dependence to more positive potentials (Fig. 7). The effects of D600 on the current-voltage relationships of both the transient and the steady-state components of I_{Ca} can be largely explained by the shift in d_∞ (cf. eqns. (4) and (5) and Fig. 6).

We have examined the effects of the calcium channel agonist BAY K8644 on I_{Ca} . BAY K8644 increases the transient component of I_{Ca} in a voltage-dependent fashion (Fig. 8). BAY K8644 shifts both d_∞ and f_∞ to more negative potentials by similar amounts. The net result is a shift in the voltage dependence of the overlap of these two curves to more negative potentials (Fig. 9). The effects of BAY K8644 on the transient component of I_{Ca} are not well explained by the shifts in d_∞ and f_∞ (see Fig. 8 and below).

Channel types

Recent reports indicate that multiple calcium channel types can co-exist in one preparation (Carbone & Lux, 1984; Bean, 1985; Nilius *et al.* 1985; Nowycky, Fox & Tsien, 1985; Tsien, Benham, Fox, Hess, Lipscombe, McCleskey, Madison & Rosenberg, 1986). These different channel types may have different conductances, different kinetics and different voltage dependences (Nowycky *et al.* 1985; Tsien *et al.* 1986). At least two channel types have been seen in cardiac muscle, 'T' and 'L' types. We have restricted our experiments to the 'L' type channel by keeping the holding potential at -50 mV although we have not searched for 'T' type channels to date.

Fig. 9. The effect of BAY K8644 on the steady-state activation (d_∞) and inactivation (f_∞) variables. *A*, the effect of BAY K8644 on steady-state activation (d_∞). ■, control ($V_h = -2.62$ mV, $k = 6.6$ mV); ◆, $1 \mu\text{M}$ -BAY K8644 ($V_h = -14.16$ mV, $k = 6.07$ mV). *B*, the effect of BAY K8644 on steady-state inactivation (f_∞). ■, control ($V_h = -6.88$ mV, $k = 9.33$ mV); ◆, $1 \mu\text{M}$ -BAY K8644 ($V_h = -18.45$ mV, $k = 5.07$ mV). *C*, the effect of BAY K8644 on the overlap of d_∞ and f_∞ .

Modes

Within a given channel type a number of stable kinetic behaviour patterns have been reported. Examining presumably the 'L' type channel, Hess *et al.* (1984) report that it may assume three kinetic modes, each with the same single-channel conductance. Nilius *et al.* (1985) find that $\gamma_{\text{ch}} = 18\text{--}25$ pS in 100 mM-external barium at 22 °C, similar to the results of Cavalie *et al.* (1983), McDonald *et al.* (1986) and Reuter, Stevens, Tsien & Yellen (1982). We have found that the transient and steady-state components of I_{Ca} can be fairly well described by d_{∞} and f_{∞} as presented in the Results section. Modulation of I_{Ca} by D600 also seems reasonably well explained by an analysis involving d_{∞} and f_{∞} . The relative conductance g_r that we use is equal to $W\gamma_{\text{ch}} n$. The single-channel conductance is thought to be invariant in modal changes. There are many possible ways to explain the dependence of I_{Ca} on voltage. For example, there could be time- and voltage-dependent changes in modal behaviour that are altered by drug, temperature and permeant ion. It is therefore of interest to note that the steady-state component of I_{Ca} is well fitted by this extremely simple model (only one free parameter, g_r) under control conditions and when D600 is applied. The largest deviations are observed at positive potentials in the presence of BAY K8644 during the transient portion of I_{Ca} . As suggested earlier this may reflect the failure of the assumption that the transition of d_0 to d_{∞} is extremely fast compared to the transition of f_0 to f_{∞} . But this may be testable in future experiments that examine the kinetics of activation as well as those of inactivation. An important observation comes during the BAY K8644 experiments where the g_r value in BAY K8644 is about twice that of control. Assuming that γ_{ch} and n are invariant, W must have increased by a factor of 2. The increase in this weighting factor is similar to the increase in the mean open time reported during the application of 1 μM -BAY K8644 and attributed to a change in modal behaviour of the calcium channel (Hess *et al.* 1984).

Calcium-dependent versus voltage-dependent inactivation

Much evidence has developed showing that in mammalian heart preparations the calcium current inactivates with maintained depolarization and that the inactivation may be ascribed to at least two processes. Calcium-dependent as well as voltage-dependent inactivation has been demonstrated in calf Purkinje fibres (Kass & Sanguinetti, 1984; Lee *et al.* 1985) and in single ventricular myocytes (Mitchell *et al.* 1983; Josephson *et al.* 1984; Lee *et al.* 1985). We have examined the experiments shown in this paper for evidence of calcium-dependent inactivation. The presumed reduction of intracellular calcium concentration by D600 is not associated with a decrease of inactivation rate constant (see our Fig. 6, and Fig. 5 from Lee & Tsien, 1983). The decrease in I_{Ca} upon the application of D600 may therefore reflect the increased closed times of the single channel in the presence of D600 seen by Cavalie *et al.* (1985) as noted by Lee *et al.* (1985). Furthermore, the calcium channel agonist BAY K8644 leads to an increase in I_{Ca} over a wide voltage range (-40 to $+5$ mV), as shown in our Fig. 8C, and presumably leads to an increase in intracellular calcium concentration. Nevertheless, there is no significant change in the time constant of inactivation of I_{Ca} over this voltage range (see our Fig. 8B). This raises questions

about the interpretation of the experiments designed to test for calcium-dependent inactivation and raises the possibility that the alterations of inactivation of I_{Ca} may not depend on changes in intracellular calcium concentration in any simple manner.

Significance of the calcium 'window current'

The presence of a steady-state component of I_{Ca} is implied by previous measurements of d_{∞} and f_{∞} (Brown *et al.* 1984; Josephson *et al.* 1984) and by single-channel measurements (Cavalié *et al.* 1983; McDonald *et al.* 1986). We have shown that the voltage dependence of the calcium 'window current' can be adequately accounted for by the voltage dependence of d_{∞} and f_{∞} . We have not taken into account the voltage dependence of the single-channel conductance (γ_{ch}) or the time dependence of changes in d , both of which are not adequately known under the conditions of our experiments. However, in 50 mM extracellular calcium (Cavalié *et al.* 1983; Hess, Lansman & Tsien, 1986) or 90 mM extracellular barium (Cavalié *et al.* 1983; McDonald *et al.* 1986) γ_{ch} is fairly constant over the potentials we investigated.

The marked variation in rat and guinea-pig action potential shape was attributed in part to variations in I_{Ca} in these species (Josephson *et al.* 1984). Similarly the variation of action potential shape in neonatal rat heart cells brought about by D600 or BAY K8644 application is consistent with changes in I_{Ca} . These findings suggest that modulation of I_{Ca} and particularly the calcium 'window current' by investigational and therapeutic agents can have profound effects not only on the duration of the electrical signal but also on calcium influx.

We thank M. B. Cannell, C. G. Nichols and J. R. Berlin for discussion of this work and comments on this manuscript, and K. E. MacEachern for technical assistance. This work has been supported by the National Institutes of Health (HL25675) and the American and Maryland Heart Associations. The work was carried out during the tenure of an Established Investigator Award supported by the American and Maryland Heart Associations (W.J.L.). N. M. C. is grateful for fellowship support from the Pharmaceutical Manufacturers Association Foundation.

REFERENCES

- ATTWELL, D., COHEN, I., EISNER, D., OHBA, M. & OJEDA, C. (1979). The steady-state TTX-sensitive ('window') sodium current in cardiac Purkinje fibres. *Pflügers Archiv* **379**, 137-142.
- BEAN, B. P. (1984). Nitrendipine block of cardiac calcium channels: high affinity binding to the activated state. *Proceedings of the National Academy of Sciences of the U.S.A.* **81**, 6388-6392.
- BEAN, B. P. (1985). Two kinds of calcium channels in canine atrial cells. *Journal of General Physiology* **86**, 1-30.
- BEZANILLA, F. (1985). A high capacity data recording device based on a digital audio processor and a video cassette recorder. *Biophysical Journal* **47**, 437-441.
- BROWN, H. F., KIMURA, J., NOBLE, D., NOBLE, S. & TAUPIGNON, A. (1984). The slow inward current, i_{sl} , in the rabbit sino-atrial node investigated by voltage clamp and computer simulation. *Proceedings of the Royal Society B* **222**, 305-328.
- BYERLY, L. & HAGIWARA, S. (1982). Calcium currents in internally perfused nerve cell bodies of *Limnea stagnalis*. *Journal of Physiology* **322**, 503-528.
- CARBONE, E. & LUX, H. D. (1984). A low voltage-activated fully inactivating Ca channel in vertebrate sensory neurons. *Nature* **310**, 501-502.
- CAVALIÉ, A., OCHI, R., PELZER, D. & TRAUTWEIN, W. (1983). Elementary currents through Ca^{2+} channels in guinea pig myocytes. *Pflügers Archiv* **398**, 284-297.

- CAVALIE, A., PELZER, D. & TRAUTWEIN, W. (1985). Modulation of the gating properties of single calcium channels by D600 in guinea-pig ventricular myocytes. *Journal of Physiology* **358**, 59P.
- COHEN, N. M. & LEDERER, W. J. (1986). Steady-state kinetic parameters of the calcium current (I_{Ca}) in neonatal rat single cardiac myocytes. *Biophysical Journal* **49**, 175a.
- COLATSKY, T. J. (1982). Mechanism of action of lidocaine and quinidine on action potential duration in rabbit cardiac Purkinje fibres: An effect on steady-state sodium currents. *Circulation Research* **50**, 17-27.
- COLQUHOUN, D., NEHER, E., REUTER, H. & STEVENS, C. F. (1981). Inward current activated by intracellular Ca in cultured cardiac cells. *Nature* **294**, 752-754.
- FENWICK, E. M., MARTY, A. & NEHER, E. (1982). Sodium and calcium channels in bovine chromaffin cells. *Journal of Physiology* **331**, 599-635.
- GADSBY, D. C., KIMURA, J. & NOMA, A. (1985). Voltage dependence of Na/K pump current in isolated heart cells. *Nature* **315**, 63-65.
- HAMILL, O. P., MARTY, A., NEHER, E., SAKMANN, B. & SIGWORTH, F. J. (1981). Improved patch-clamp techniques for high-resolution current recording from cells and cell-free membrane patches. *Pflügers Archiv* **391**, 85-100.
- HESS, P., LANSMAN, J. B. & TSIEN, R. W. (1984). Different modes of Ca channel gating behaviour favoured by dihydropyridine Ca agonists and antagonists. *Nature* **311**, 538-544.
- HESS, P., LANSMAN, J. B. & TSIEN, R. W. (1986). Calcium channel selectivity for divalent and monovalent cations: Voltage and concentration dependence of single channel current in ventricular heart cells. *Journal of General Physiology* **88**, 239-319.
- HUME, J. R. (1985). Comparative interactions of organic Ca^{++} channel antagonists with myocardial Ca^{++} and K^+ channels. *Journal of Pharmacology and Experimental Therapeutics* **234**, 134-140.
- ISENBERG, G. & KLOCKNER, U. (1982). Calcium currents of isolated bovine ventricular myocytes are fast and of large amplitude. *Pflügers Archiv* **395**, 30-41.
- JOSEPHSON, I. R., SANCHEZ-CHAPULA, J. & BROWN, A. M. (1984). A comparison of calcium currents in rat and guinea pig single ventricular cells. *Circulation Research* **54**, 144-156.
- JOURDAN, PH. (1984). Extrasystolic action potential and contraction in newborn rat myocardium. *Developmental Pharmacology and Therapeutics* **7**, suppl. 1, 194-200.
- KASS, R. S. & SANGUINETTI, M. C. (1984). Inactivation of calcium channel current in the calf cardiac Purkinje fiber. *Journal of General Physiology* **84**, 705-726.
- KASS, R. S. & TSIEN, R. W. (1975). Multiple effects of calcium antagonists on plateau currents in cardiac Purkinje fibers. *Journal of General Physiology* **66**, 169-192.
- KASS, R. S. & TSIEN, R. W. (1976). Control of action potential duration by calcium ions in cardiac Purkinje fibers. *Journal of General Physiology* **67**, 599-617.
- KIMURA, J., NOMA, A. & IRISAWA, H. (1986). Na-Ca exchange current in mammalian heart cells. *Nature* **319**, 596-597.
- LANGER, G. A., BRADY, A. J., TAN, S. W. & SERENA, S. D. (1975). Correlation of the glycoside response, the force staircase, and the action potential configuration in the neonatal rat heart. *Circulation Research* **36**, 744-752.
- LEE, K. S., MARBAN, E. & TSIEN, R. W. (1985). Inactivation of calcium channels in mammalian heart cells: joint dependence on membrane potential and intracellular calcium. *Journal of Physiology* **364**, 395-411.
- LEE, K. S. & TSIEN, R. W. (1982). Reversal of current through calcium channels in dialysed single heart cells. *Nature* **297**, 498-501.
- LEE, K. S. & TSIEN, R. W. (1983). Mechanism of calcium channel blockade by verapamil, D600, diltiazem and nitrendipine in single dialysed heart cells. *Nature* **302**, 790-794.
- LEE, K. S. & TSIEN, R. W. (1984). High selectivity of calcium channels in single dialysed heart cells of the guinea-pig. *Journal of Physiology* **354**, 253-272.
- MCDONALD, T. F., CAVALIE, A., TRAUTWEIN, W. & PELZER, D. (1986). Voltage-dependent properties of macroscopic and elementary calcium channel currents in guinea pig ventricular myocytes. *Pflügers Archiv* **406**, 437-448.
- MCDONALD, T. F., PELZER, D. & TRAUTWEIN, W. (1980). On the mechanism of slow calcium channel block in heart. *Pflügers Archiv* **385**, 175-179.

- McDONALD, T. F., PELZER, D. & TRAUTWEIN, W. (1984). Cat ventricular muscle treated with D600: characteristics of block and unblock. *Journal of Physiology* **352**, 217–241.
- MITCHELL, M. R., POWELL, T., TERRAR, D. A. & TWIST, V. W. (1983). Characteristics of the second inward current in cells isolated from rat ventricular muscle. *Proceedings of the Royal Society B* **219**, 447–469.
- NILIUS, B., HESS, P., LANSMAN, J. B. & TSIEN, R. W. (1985). A novel type of cardiac calcium channel in ventricular cells. *Nature* **316**, 443–446.
- NILIUS, B. & ROEDER, A. (1985). Direct evidence of Ca-sensitive inactivation of slow inward channels in frog atrial myocardium. *Biomedica biochimica acta* **44**, 1151–1161.
- NOWYCKY, M. C., FOX, A. P. & TSIEN, R. W. (1985). Three types of neuronal calcium channels with different calcium agonist sensitivity. *Nature* **316**, 440–443.
- REUTER, H., STEVENS, C. F., TSIEN, R. W. & YELLEN, G. (1982). Properties of single calcium channels in cardiac cell culture. *Nature* **297**, 501–504.
- SANGUINETTI, M. C. & KASS, R. S. (1984*a*). Voltage-dependent block of calcium channel current in the calf cardiac Purkinje fiber by dihydropyridine calcium channel antagonists. *Circulation Research* **55**, 336–348.
- SANGUINETTI, M. C. & KASS, R. S. (1984*b*). Regulation of cardiac calcium channel current and contractile activity by the dihydropyridine Bay K 8644 is voltage-dependent. *Journal of Molecular and Cellular Cardiology* **16**, 667–670.
- SANGUINETTI, M. C., KRAFTE, D. S. & KASS, R. S. (1986). Voltage dependent modulation of Ca channel current in heart cells by Bay K 8644. *Journal of General Physiology* **88**, 369–392.
- SCHREINER, W., KRAMER, M., KRISCHER, S. & LANGSAM, Y. (1985). Nonlinear least squares fitting. *PC Tech Journal* **3**, 170–190.
- SHEU, S.-S. & LEDERER, W. J. (1985). Lidocaine's negative inotropic and antiarrhythmic actions: Dependence on shortening of action potential duration and reduction of intracellular sodium activity. *Circulation Research* **57**, 578–590.
- SIEGELBAUM, S. A. & TSIEN, R. W. (1980). Calcium-activated transient outward current in calf cardiac Purkinje fibres. *Journal of Physiology* **299**, 485–506.
- TSIEN, R. W., BENHAM, C. D., FOX, A. P., HESS, P., LIPSCOMBE, D., MCCLESKEY, E. W., MADISON, D. V. & ROSENBERG, R. L. (1986). Multiple types of calcium channel in neurons and muscle cells and their modulation by neurotransmitters. *Journal of General Physiology* **88**, 1a.